

Filtering spin with tunnel-coupled electron wave guides

M. Governale, D. Boese, U. Zülicke, C. Schroll

Institut für Theoretische Festkörperphysik, Universität Karlsruhe, D-76128 Karlsruhe, Germany

Spintronics is an emerging field of semiconductor electronics where the electron's spin is exploited as well as its charge¹. Operation of spintronic devices requires the ability to create spin-polarized charge carriers in nonmagnetic semiconductors. Using Zeeman splitting of spin states in a magnetic field turns out to be impractical for spin filtering in real applications. More promising approaches employ hybrid structures² with metallic^{3–5} or semiconducting^{6–8} magnetic contacts. However, fabrication of these structures poses material-science challenges⁹ and may require rather complicated chip design. Achieving spin filtering by means of intrinsic spin-dependent effects in semiconductors is therefore highly desirable¹⁰. Here we propose a spin-filtering device based on the interplay of the Rashba effect¹¹ and momentum-resolved tunneling¹² between parallel electron wave guides. Spin-polarized currents are created by applying voltages or small magnetic fields. Switching between opposite spin polarizations is easily achieved. Verification of spin filtering in the device is possible via measurement of the differential tunneling conductance, which would yield the first direct observation of the Rashba effect.

The basic setup shown in Fig. 1a consists of two parallel one-dimensional (1D) electron wave guides, also called quantum wires, that are coupled via tunneling through a clean, uniform, nonmagnetic barrier of finite length L . Such a system can be realized, e.g., by quantum confinement of electrons in semiconductor heterostructures using split-gate techniques^{12,13} or

cleaved-edge overgrowth (Auslaender, O. M. & Yacoby, A. Private communication.). Electrons moving in the wave guides are 1D plane waves whose wave number k is related to their canonical momentum by $p = \hbar k$. In addition, the quantum-mechanical state of electrons is characterized by their intrinsic spin degree of freedom, which can be either up or down. Within the tunneling region, a finite quantum-mechanical probability amplitude $t_{k,k'}$ exists for electrons to leave a state with wave number k in one wire and occupy a state with wave number k' in the other wire. This fact enables current flow across the tunnel barrier when a finite voltage bias $V = V_U - V_L$ is applied. (See Fig. 1a.) Translational invariance along an extended uniform tunnel barrier implies approximate momentum conservation in a single tunneling event. More precisely¹⁴, the tunneling probability $|t_{k,k'}|^2$ exhibits a peak for $k = k'$ with height $|t|^2 L^2$ and width $2\pi/L$. The spin state of a tunneling electron remains unchanged. Hence, tunneling between parallel quantum wires is a highly wave-number-selective but entirely spin-insensitive process.

In our device, wave-number selectivity is utilized for spin filtering by means of an intrinsic coupling of the electron's spin to its momentum. Physically, such a spin-orbit coupling originates from structural inversion asymmetry¹⁵ present in quantum-confined systems. This effect, named after É. I. Rashba, renders the kinetic energy of an electron with momentum $\hbar k$ dependent on its spin state¹¹:

$$E_{k\sigma} = E_0 + \frac{\hbar^2}{2m} (k - \sigma k_{\text{so}})^2 - \Delta_{\text{so}} \quad . \quad (1)$$

Here, the spin quantum number σ distinguishes spin-up ($\sigma = 1$) and spin-down ($\sigma = -1$) electron states. The effective mass of electrons is denoted by m , E_0 is the 1D subband energy, and $\Delta_{\text{so}} = \hbar^2 k_{\text{so}}^2 / (2m)$. The strength of spin-orbit coupling can be expressed in terms of a characteristic wave number, denoted here by k_{so} . Experimental efforts^{16,17} aimed at the realization of an early proposal¹⁸ for a spin-controlled field-effect transistor established tunability of k_{so} by external gate voltages. In our device (see Fig. 1a), the voltage V_g is used to achieve different strengths of Rashba spin-orbit coupling in the two wires. In that situation, tunneling transport across the barrier provides a direct measurement of the Rashba effect. The differential tunneling conductance, calculated by us and shown in Fig. 2, provides a

direct image of the spin-resolved parabolic dispersion curves given by Eq. (1).

When a picture like Fig. 2 is obtained for the differential tunneling conductance, the double-wire system can be used for spin filtering. To simplify the explanation of its basic operational modes as a spin polarizer and a spin splitter, we consider here the special case where Rashba spin-orbit coupling is finite in the upper wire (labeled U) but vanishes in the lower wire (labeled L). Taking into account a finite subband-energy difference $\Delta E_0 = E_0^{(U)} - E_0^{(L)}$, electronic dispersion relations look like shown in Fig. 3a. Only states with energies below $E_0^{(U)} + \varepsilon_{F,U}$ in the upper wire (below $E_0^{(L)} + \varepsilon_{F,L}$ in the lower wire) are occupied with electrons. Due to wave-number selectivity, tunneling can only occur for electron states with wave number close to a point where the dispersion curves of the two wires cross¹⁴. In the case depicted in Fig. 3a, no such crossings occur for states that are occupied in either one of the two wires, and no tunneling current can flow. All electrons injected into the upper wire from reservoirs 1 and 2 remain in the upper wire (Fig. 1b). This situation can change when a magnetic field B is applied perpendicular to the plane of the two wires. It leads to a relative shift¹⁴ of the two wires' dispersion curves in wave-number direction by $p_B = -eBd/\hbar$, where $-e$ is the electron charge, and d the wire separation. For particular values of magnetic field, namely whenever the condition

$$p_B = \frac{\pi}{2} (\gamma n_U - \gamma' n_L) - \sigma k_{so} \quad (2)$$

is satisfied with $\gamma, \gamma' = \pm 1$ and $n_{U(L)}$ denoting electron density in the upper (lower) wire, tunneling is enabled for electrons in spin state σ . Simultaneous tunneling of electrons with opposite spin will be prohibited for high enough wave-number selectivity, i.e., if $\pi/L \ll k_{so}$. The case corresponding to $\gamma = \gamma' = +1$ is depicted in Fig. 3b. In that situation, a spin-polarized current of electrons from reservoir 1 reaches reservoir 4. As shown in Fig. 1c, it is compensated globally by the current of spin-up electrons from reservoir 2 that can only reach reservoir 1. Using the standard scattering-theory formalism¹⁹ for calculating electron transport, we have obtained the linear conductance for tunneling across the barrier. Our results, given in Fig. 4a, show the four resonances determined by solutions of Eq. (2) which exhibit almost perfect spin polarization of the tunneling current. We emphasize that the

applied magnetic field, used here simply to tune wave-number selectivity, is typically much smaller than the field required to achieve spin-filtering from Zeeman splitting. Tuning between the four resonances allows the double-quantum-wire system to be used as a switchable spin-polarizer. Analyzing the resonance condition given by Eq. (2) from a fundamental point of view, we realize that this is possible because Rashba spin-orbit coupling acts essentially like a spin-dependent orbital magnetic field.

Intriguingly, spin-polarized currents can be created in our device without applying any magnetic field at all. Instead, a finite bias voltage V can be used to induce a relative shift $-eV$ of the two wire's dispersion curves in energy direction²⁰. This way, coincidences of the two wire's dispersion curves are created for electron states with spin σ and wave number k satisfying

$$eV = \Delta E_0 - \frac{\hbar^2}{m} k_{\text{so}} \sigma k \quad . \quad (3)$$

If such a state is occupied by an electron in one wire and empty in the other one, it will contribute to the tunneling current. A situation where current flow is made possible by the applied voltage is depicted in Fig. 3c. Tunneling is simultaneously enabled for electrons having opposite spin and wave number, which will end up in opposite leads of the wire they have tunneled into. For large enough wave-number selectivity, tunneling for a particular spin species turns out to occur, if at all, only for wave numbers of one sign. As a result, currents flowing in the leads of the double-wire device are fully spin-polarized. This is seen in Fig. 4b for a particular set of parameters. Currents in leads 1 and 3 have the same spin polarization, which is opposite to that in leads 2 and 4. Selection of spin-up or spin-down polarization for currents in leads 1 and 3 (2 and 4) is possible simply by adjusting the voltage. While no global spin imbalance is created, wave-number selectivity leads to a redistribution of spin-polarized currents between the four leads. Thereby, spin filtering is possible without any magnetic or exchange fields. Note that wave-number selectivity provides the most direct way to utilize the Rashba effect for spin filtering. As a result, our device offers crucial advantages²¹ over the one proposed in Ref. 10 which is based on energy selectivity.

Three mechanisms limit functionality of a real double-wire system as a spin-filtering

device. First, wave-number selectivity is reduced by disorder. However, the successful measurement of 1D dispersion curves for parallel quantum wires in GaAlAs heterostructures (Auslaender, O. M. & Yacoby, A. Private communication.) demonstrates the possibility to achieve sufficient wave-number selectivity using present-day technology. While this particular system cannot be used for spin filtering due to its negligible Rashba effect, similar structures could be created in more suitable materials. Second, quantum wires are really multi-channel 1D wave guides for electrons. Spin-orbit coupling induces mixing between these channels (subbands), which was neglected in our discussion so far. Detailed analysis¹⁸ shows that subband mixing can be safely neglected as long as the energy difference between consecutive quasi-1D subbands is much larger than Δ_{so} . In present-day samples, this requirement is easily met for realistic values^{16,17} of k_{so} . Finally, our conclusions apply at temperatures T low enough such that smearing of the Fermi function does not substantially decrease wave-number selectivity. The relevant criterion $k_{\text{B}}T \lesssim \hbar^2 k_{\text{so}} k_{\text{F,L}}/m$ translates, for typical sample parameters, into $T \lesssim 10$ K. This temperature range is routinely accessible in semiconductor-research laboratories where our basic design for a spin-filtering device could be demonstrated.

Experimental tests for the successful operation of our device as spin polarizer or spin splitter could be based on the usual spin-detection mechanisms, applied to currents leaving or entering any of the four leads. For example, ferromagnetic contacts can serve as spin analyzers, or spin polarization of charge carriers could be measured optically^{5–8}. Results of such experiments will be determined not only by the efficiency of spin filtering in the double-wire system but also by spin-equilibration processes in the leads. An equally significant test is provided by measurement of the differential tunneling conductance as a function of magnetic field and transport voltage. Clearly resolved Rashba-split dispersion curves, as shown in Fig. 2, prove sufficient wave-number selectivity for addressing different spin states and constitute therefore the decisive experimental demonstration of spin filtering in our device.

1. Prinz, G. A. Magnetoelectronics. *Science* **282**, 1660-1663 (1998).
2. Prinz, G. A. Hybrid Ferromagnetic-Semiconductor Structures. *Science* **250**, 1092-1097 (1990).
3. Hammar, P. R., Bennet, B. R., Yang, M. J. & Johnson, M. Observation of spin injection at a ferromagnet-semiconductor interface. *Phys. Rev. Lett.* **83**, 203-206 (1999).
4. Gardelis, S., Smith, C. G., Barnes, C. H. W., Linfield, E. H. & Ritchie, D. A. Spin-valve effects in a semiconductor field-effect transistor: A spintronic device. *Phys. Rev. B* **60**, 7764-7767 (1999).
5. Zhu, H. J. *et al.* Room-temperature spin injection from Fe into GaAs. *Phys. Rev. Lett.* **87**, 016601 (2001).
6. Oestreich, M. *et al.* Spin injection into semiconductors. *Appl. Phys. Lett.* **74**, 1251-1253 (1999).
7. Fiederling, R. *et al.* Injection and detection of a spin-polarized current in a light-emitting diode. *Nature* **402**, 787-790 (1999).
8. Ohno, Y. *et al.* Electrical spin injection in a ferromagnetic semiconductor heterostructure. *Nature* **402**, 790-792 (1999).
9. Schmidt, G., Ferrand, D., Molenkamp, L. W., Filip, A. T. & van Wees, B. J. Fundamental obstacle for electrical spin injection from ferromagnetic metal into a diffusive semiconductor. *Phys. Rev. B* **62**, R4790-4793 (2000).
10. Kiselev, A. A. & Kim, K. W. T-shaped ballistic spin filter. *Appl. Phys. Lett.* **78**, 775-777 (2001).
11. Bychkov, Yu. A. & Rashba, É. I. Properties of a 2D electron gas with lifted spectral degeneracy. *JETP Lett.* **39**, 78-81 (1984).

12. Eugster, C. C., del Alamo, J. A., Rooks, M. J. & Melloch, M. R. One-dimensional to one-dimensional tunneling between electron wave guides. *Appl. Phys. Lett.* **64**, 3157-3159 (1994).
13. Thomas, K. J. *et al.* Controlled wave-function mixing in strongly coupled one-dimensional wires. *Phys. Rev. B* **59**, 12252-12255 (1999).
14. Boese, D., Governale, M., Rosch, A. & Zülicke, U. Mesoscopic effects in tunneling between parallel quantum wires. *Phys. Rev. B* **64**, 085315 (2001).
15. Winkler, R. Rashba spin splitting in two-dimensional electron and hole systems. *Phys. Rev. B* **62**, 4245-4248 (2000).
16. Nitta, J., Akazaki, T., Takayanagi, H. & Enoki, T. Gate Control of Spin-Orbit Interaction in an Inverted $\text{In}_{0.53}\text{Ga}_{0.47}\text{As}/\text{In}_{0.52}\text{Al}_{0.48}\text{As}$ Heterostructure. *Phys. Rev. Lett.* **78**, 1335-1338 (1997).
17. Grundler, D. Large Rashba Splitting in InAs Quantum Wells due to Electron Wave Function Penetration into the Barrier Layers. *Phys. Rev. Lett.* **84**, 6074-6077 (2000).
18. Datta, S. & Das, B. Electronic analog of the electro-optic modulator. *Appl. Phys. Lett.* **56**, 665-667 (1990).
19. Büttiker, M. Symmetry of electrical conduction. *IBM J. Res. Dev.* **32**, 317-334 (1988).
20. In general, charging and exchange-correlation effects in the wires renormalize the voltage-induced shift of their dispersion curves. This can be taken into account straightforwardly and does not alter functionality of our device as a spin-splitter.
21. The most important advantage is that spin filtering occurs in our setup when the transmission into output channels is maximal. This is different in the T-junction device of Ref. 10 where resonance with quasi-zerodimensional bound states is essential to achieve appreciable spin filtering but, at the same time, results in almost complete backscattering. Furthermore, in contrast to the double-wire device proposed here,

spin filtering in the T-junction is large only in the limit of small spin-orbit coupling where delicate voltage control is required for tuning into resonance or switch spin states in the output channels. Finally, the complex interplay of the many parameters characterizing the T-junction device prevents a straightforward device optimization that is clearly possible in our conceptually simpler system.

Acknowledgments

This work was supported by Deutsche Forschungsgemeinschaft (Sonderforschungsbereich 195, Graduiertenkolleg "Kollektive Phänomene im Festkörper"). We thank G. Schön for useful discussions and a critical reading of the manuscript.

Correspondence and requests for materials should be addressed to U.Z. (e-mail: ulrich.zuelicke@phys.uni-karlsruhe.de).

Figure 1 Schematic picture of spin-filtering device and spin-polarized currents. **a**, Two parallel quantum wires, labeled 'U' and 'L', are each connected to reservoirs having equal chemical potential V_U and V_L . A gate voltage V_g is used to control the intrinsic Rashba spin-orbit coupling of electrons in the two wires. Within the blue-shaded region of length L , electrons can tunnel between the wires. Uniformity of the tunnel barrier leads to wave-number selectivity of tunneling processes. Together with spin-orbit coupling, this results in spin-polarized currents in the leads. **b**, Reservoir 1 (2) injects right-moving (left-moving) electrons into the upper wire. When wave-number selectivity and Pauli blocking prevents their tunneling into the lower wire, these are absorbed by the opposite reservoir, and no net current is flowing through either wire. We show only currents for spin-up electrons. **c**, The interplay of spin-orbit coupling and wave-number selectivity enables tunneling only for right-moving spin-up electrons. As a result, a spin-polarized current is flowing through the barrier, effectively, from reservoir 2 to reservoir 4. All other currents are compensated and not shown.

Figure 2 Color plot of the differential conductance for tunneling across the barrier, shown in arbitrary units, as function of the transport voltage V and a magnetic field B perpendicular to the plane of the wires. The field strength B is absorbed, together with wire separation d and electron charge $-e$, in the parameter $p_B = -eBd/\hbar$. Red and blue resonance features map out electronic band dispersion curves in the two wires, with eV and p_B playing the rôles of energy and wave number, respectively. Appearance of two sets of identical parabolic curves that are shifted in magnetic-field direction are the unambiguous signature of Rashba spin-orbit coupling of different strength in the two wires. Hence, the measurement of the differential conductance in our setup allows a spectroscopic observation of the Rashba effect. Furthermore, resolving spin-split electron bands proves feasibility of spin filtering in the double-wire device. Note that the two crossing points exhibited for zero p_B correspond to situations where the double-wire device acts as a spin splitter. (See Figs. 3c and 4b.) For simplicity, it was assumed in our calculation that the strength of Rashba spin-orbit coupling is finite in the upper wire but vanishes in the lower wire. We then use the lower wire's Fermi wave number $k_{F,L}$ and Fermi energy $\varepsilon_{F,L}$ as wave-number and energy units, respectively. (Fermi wave number and electron density of the lower wire are related via $k_{F,L} = \pi n_L/2$.) Parameters used in the calculation are $\Delta E_0 = 0.15 \varepsilon_{F,L}$, $k_{so} = 0.1 k_{F,L}$, $L = 100/k_{F,L}$, $|t| = \varepsilon_{F,L} \cdot \pi/1000$. Our calculation is based on perturbation theory in tunneling and neglects charging as well as exchange-correlation effects in the wires. The finite width of resonance features in the plot is due to the finite length L of the tunnel barrier.

Figure 3 Tunability of energy dispersion relations for electrons in the wires by magnetic field and transport voltage. **a**, Equilibrium situation. Due to the Rashba effect, the dispersion curves for spin-up and spin-down electrons in the upper wire are shifted horizontally by $2k_{so}$. In the lower wire where spin-orbit coupling is assumed to be absent, energy dispersions are spin-degenerate. A finite mismatch ΔE_0 of one-dimensional subband energies is taken into account. Only states below the chemical potential, indicated for each wire by dashed lines, are occupied by electrons. **b**, Device operation as a spin polarizer. Tuning wave-

number selectivity by a magnetic field B , tunneling is selectively enabled for right-moving electrons with spin up. **c**, Device operation as a spin splitter. Application of a finite voltage V simultaneously enables tunneling for left-moving spin-down electrons and right-moving spin-up electrons.

Figure 4 Tunneling transport characteristics, calculated exactly using scattering theory (a) and perturbatively (b) as explained in Ref. 14. **a**, Total linear tunneling conductance through the barrier $G^{\text{tot}} = G_{\uparrow} + G_{\downarrow}$ (left axis) and spin-polarized conductance $G^{\text{pol}} = G_{\uparrow} - G_{\downarrow}$ (right axis) vs. magnetic field B . Resonances with definite spin polarization occur at values of the magnetic field determined by Eq. (2). Data shown are for $\Delta E_0 = 0.1 \varepsilon_{\text{F,L}}$, $k_{\text{so}} = 0.05 k_{\text{F,L}}$, $L = 200/k_{\text{F,L}}$, $|t| = \varepsilon_{\text{F,L}} \cdot \pi/1000$. **b**, Currents in all the leads are spin-polarized when operating the device in spin-splitting mode (Fig. 3c). We define total and spin currents entering lead j by $I_j^{\text{tot}} = I_j^{\uparrow} + I_j^{\downarrow}$ and $I_j^{\text{pol}} = [I_j^{\uparrow} - I_j^{\downarrow}] \text{sgn}(I_j^{\text{tot}})$, respectively. In the spin-splitter mode, we have $I_4^{\text{tot}} = I_3^{\text{tot}} = -I_2^{\text{tot}} = -I_1^{\text{tot}}$. We show I_3^{tot} vs. transport voltage $V = V_{\text{U}} - V_{\text{L}}$ (dotted curve). Due to wave-number selectivity, it is appreciable only in finite ranges of voltage where states near points of coincidence for the wires' dispersion curves are occupied in one wire but empty in the other one. Within these voltage intervals, total current in each lead is practically always 100% spin polarized. This is seen, e.g., from comparing I_3^{tot} with I_3^{pol} (solid curve) and I_4^{pol} (dashed curve). Data shown are calculated for $\Delta E_0 = 0.15 \varepsilon_{\text{F,L}}$, $k_{\text{so}} = 0.1 k_{\text{F,L}}$, $L = 100/k_{\text{F,L}}$, $|t| = \varepsilon_{\text{F,L}} \cdot \pi/1000$, $B = 0$. Current is measured in units of $I_0 = 2e\pi|t|^2L^2/(\hbar^3v_{\text{F,L}}v_{\text{F,U}})$, where $v_{\text{F,U}}$ ($v_{\text{F,L}}$) is the Fermi velocity in the upper (lower) wire.

FIGURES

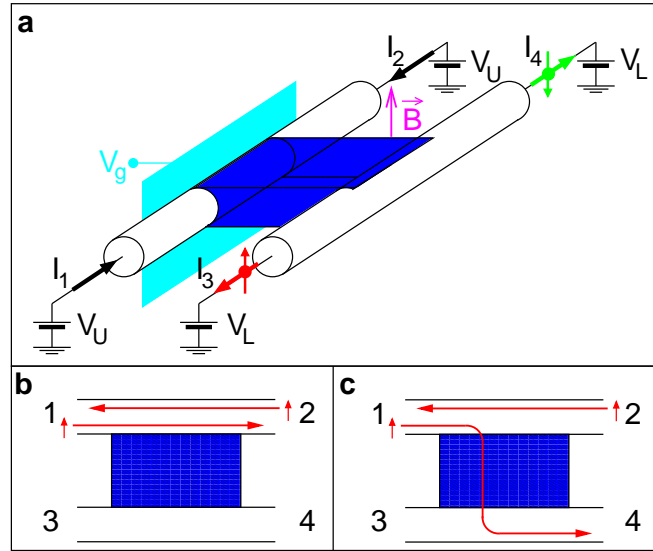


FIG. 1.

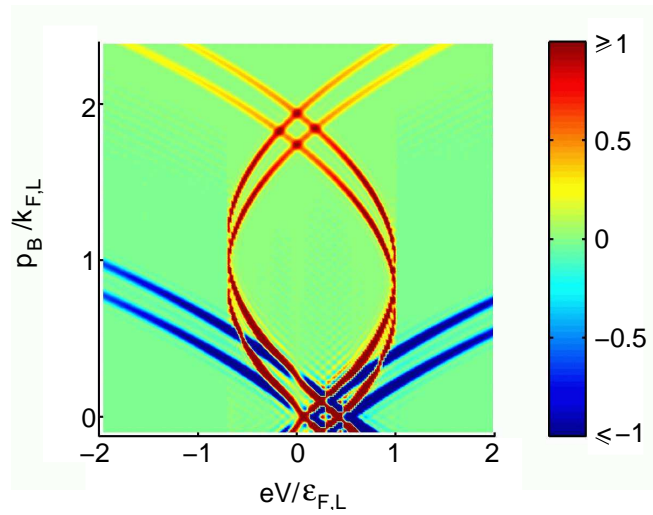


FIG. 2.

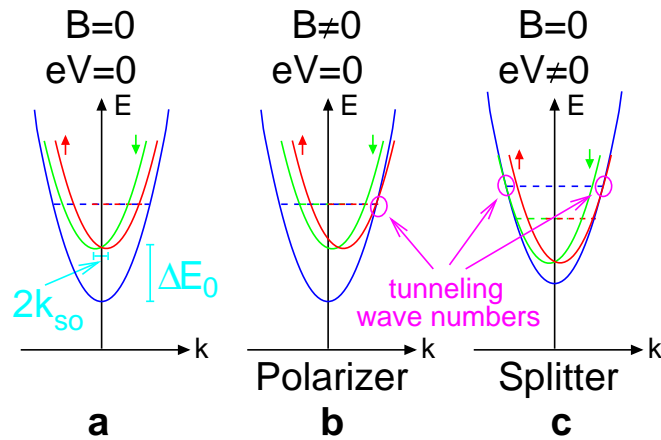


FIG. 3.

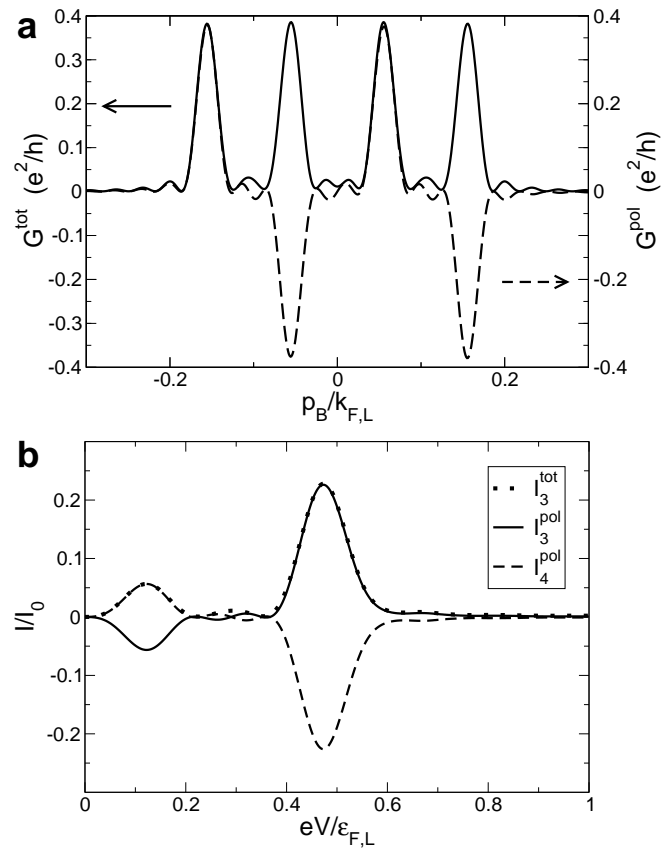


FIG. 4.